A SATURATION INTERPRETATION MODEL for the DIELECTRIC CONSTANT OF SHALY SANDS

M. T. Myers

INTRODUCTION

A long standing goal in log interpretation has been to accurately estimate oil saturation in fresh water shaly sands. In fresh water shaly sands the resistivity is determined to a large extent by the clays. Quantifying shaliness has been limited to correlations with logs such as the gamma ray, sonic, or differences in the neutron and density porosity logs.[1] This type of correlation is based on different physics than the conductivity. This means that the correlations are of limited applicability other than in the specific area where they are developed. Recently there has been considerable interest in applying dielectric measurements to interpret oil saturation but this has mostly been directed at texture effects.[2,3]

The dielectric response of clays however should be a very useful interpretation tool since it is directly related to physics controlling the clay conductivity. Particularly useful in the case of fresh water shaly sands. For fresh formation waters the dielectric response is insensitive to the brine resistivity. This allows a two frequency measurement of the dielectric constant to be interpreted independent of salinity and pore geometry for shaliness and saturation.

PURPOSE AND SCOPE

In this paper the dielectric constant of shaly sands is investigated. A model has been developed in the 1 Mhz to 1 GHz frequency range. The equation associated with this model involves the same parameters as those governing the resistivity response of shaly sands. The frequency independent high frequency limit is discussed first. Then the effects of porosity and shaliness on the dielectric constant are then examined at fixed frequency and salinity by comparing two groups of data each at nearly the same porosity. The salinity and frequency dependence of the derived parameters are then discussed for an expanded data set. The saturation dependent data and model are then discussed in the context of the brine saturated model.

The Dielectric Model: A Superposition of Terms

The dielectric constant of shaly sands is dominated by contributions from three different physical mechanisms. The dielectric constant of the bulk materials dominates at high frequencies. At lower frequencies clay minerals contribute through the polarization of the double layer and ionic conduction adds a term through the Maxwell-Wagner effect. This is summarized by a simple addition of terms:

ε_{hfl} the high frequency limit. $\Delta\varepsilon_c$ is the contribution from the

1

$$\varepsilon = \varepsilon_{hfl} + \Delta\varepsilon_c + \Delta\varepsilon_g \tag{1}$$

clay minerals in the rock sample. $\Delta\varepsilon_g$ is the contribution due to the pore geometry, which is determined by variations in the sample conductivity. In the frequency range relevant to this paper, 1 Mhz to 1.3 Ghz, $\Delta\varepsilon_c$ and $\Delta\varepsilon_g$ are frequency dependent (dispersive) while ε_{hfl} is not. Throughout the paper a Δ will signify a dielectric dispersion term. The dispersive terms arise because of interactions between the rock fabric and the brine. A vacuum dried sample shows no frequency dependence in this frequency range.

The dielectric constant is assumed to be the sum of the contributions from the individual mechanisms. This is a simplification because it doesn't allow for interactions between the different polarization mechanisms. However, because of the different physical mechanisms involved the approximation is thought to be very good.

The High Frequency Limit

The real part of the dielectric constant is conveniently divided into two terms. A frequency dependent term which decreases with increasing frequency and its asymptotic limit. The dispersive effects are isolated by subtracting this high frequency limit. This limit is fit extremely well by a two component mixing law, the Hanai-Bruggeman equation:[4]

$$\left[\frac{\varepsilon_{hfl} - \varepsilon_b}{\varepsilon_m - \varepsilon_b}\right] = \varphi \left[\frac{\varepsilon_{hfl}}{\varepsilon_m}\right]^L \tag{2}$$

The value used for ε_m the dielectric constant of the matrix is 4.4. This is the value of the dielectric constant of amorphous quartz. ε_b the dielectric constant of the brine is 77 for .01 Molal brine at 28°C. Dielectric data at 1.2 Ghz and the fit to equation (2) using these parameters are shown in Figure 1. The dielectric data are network analyzer measurements at 1.2 GHz on a variety of clastic samples which ranged from 5% to 20% in porosity and cation exchange capacities from 0.0 to 5.0 meq/100 gms shaliness. Within the accuracy of our data no effect has been found on the high frequency limit due to shaliness.

The depolarization ratio, L, in equation (2) is the fraction of the surface area of the grains perpendicular to applied electric field. This is the only value fit to the data in equation (2). The best fit value for the clastic sample set is 1/3. This value provided a good fit at all salinities. In the absence of dielectric measurements this value provides a good estimate for L.

The salinity dependence of the high frequency limit is modeled by using salinity dependent parameters. The dielectric constant of

2

the quartz matrix is still 4.4. The dielectric constant of the brine now depends on salinity and temperature. Using the empirical equations of Styrogyn the dielectric constant of NaCl brine is given by:[5]

$$\varepsilon_b = \varepsilon_b(T) \, A(N) \qquad (3)$$

where

$$\varepsilon_b(T) = 87.74 - .4008 \, T + 9.398 \, 10^{-4} \, T^2 + 1.410 \, 10^{-6} \, T^3 \qquad (4)$$

$$A(N) = 1.000 - .2551 \, N + 5.151 \, 10^{-2} \, N^2 - 6.889 \, 10^{-3} \, N^3 \qquad (5)$$

$$N = (PPM) \, [1.707 \, 10^{-5} + 1.205 \, 10^{-8} \, (PPM) + 4.058 \, 10^{-18} \, (PPM)^2] \qquad (6)$$

T is the temperature in °C and N is the normality of the salt solution and ppm is the NaCl concentration in parts per million. equation (3) is valid up to 230,000 ppm. The graph of the dielectric constant of brine versus salinity and temperature predicted by these equations is given in Figure 2. At 28°C our measurement temperature, ε_b varies between 77 for distilled water and 60 for 1 molal brine.

These values for the parameters and equation (2) will be used to determine the high frequency limits in the data analysis described below.

Effects of Shaliness and Porosity on the Dielectric Dispersion ($\Delta\varepsilon$)

To model the clay dependence of the dielectric dispersion a new shaly sand parameter Q_{bv} is introduced. Q_{bv} is the cation exchange capacity normalized to the bulk volume of the sample. Q_{bv} (meq/ml) is given by:

$$Q_{bv} = \frac{(CEC) \, \rho_g \, (1 - \varphi)}{100} \qquad (7)$$

Where CEC is the cation exchange capacity (meq/100 gms), ϕ is the fractional porosity, and ρ_g is the grain density (gm/cc). The $\rho_g(1 - \phi)/100$ term changes the normalization of the CEC from the weight of the rock grains (meq/100 gms) to the volume of rock (meq/cc). Q_{bv} is therefore independent of sample porosity.

The the amount of polarization contributed by the clays is governed only by the number of exchange sites and not dependent upon the amount of brine present (porosity). Q_v is the concentration of cation exchange site normalized to the pore volume. Q_v is appropriate for the conductivity because it is a weighting factor between the contributions to the conductivity from the brine and the clay counter-ions.[6],[7] Because only the

3

polarization of the double layer contributes to the clay term Q_{bv} should be used rather than Q_v.

In order to test these ideas and because of the historical significance of relating Q_v to shaliness effects, fits to Q_v and Q_{bv} will be compared. Two sets of data are fit at fixed frequencies and salinity (.01 Molal). The samples in each data set are clustered around distinctly different porosities. The low porosity samples range from $\phi=.08$ to $\phi=.12$ and the high porosity samples range from $\phi=.19$ to $\phi=.23$. This allows an unambiguous determination of the effects of porosity and shaliness on the dielectric constant.

Porosity Dependence of the Clay Dispersion($\Delta \varepsilon_c$): Q_{bv} Versus Q_v

The equations to be fit to the two shaliness parameters are:

$$\Delta \varepsilon = \varepsilon_q Q_{bv} + \Delta \varepsilon_g \qquad (8)$$

$$\Delta \varepsilon = \varepsilon_q Q_v + \Delta \varepsilon_g \qquad (9)$$

Where ε_q and $\Delta \varepsilon_g$ are fitted parameters. The lack of porosity dependence in the clay terms implies that the total number of ions in the pores is not important. The concentration of clay counter-ions normalized to the sample volume determines the magnitude of this term. The formation factor F* is not involved. Polarization of the double layer is a local effect with negligible interactions over distances of several pore diameters. This is confirmed by dielectric measurements made on shales which have a large dielectric dispersion and in fact lie on the low salinity trends.

Figure 3 and Figure 4 are examples of the fits of the dielectric dispersion versus Q_v, (CEC/pore volume) and Q_{bv} (CEC/bulk volume) for the low and high porosity data sets at 47 MHz. The fitted parameters at 20 MHz, 25 MHz, 47 MHz, and 200 MHz are given in Table I. The most striking feature of the fits is the comparison of the slopes. Using Q_{bv} gives identical slopes for the high and low porosity data sets within the error bars. The regressions against Q_v give slopes which are porosity dependent. The effect due to clays on the real part of the dielectric constant is independent of the amount of brine.

This is different from the in-phase conductivity where the contribution due to the conductivity from the clays has to be weighed against the contribution due to the brine and, therefore, the weighting factor Q_v is present. Other papers have discussed a similar variation of the dielectric response with the surface to volume ratio measurements.[8] This is consistent with Q_{bv} since there is a correlation between shaliness as measured by the CEC and surface area.[9] However the clay response is dominated by polarization of the double layer, not by interfacial phenomena.

4

The correlation coefficients for these fits are also given in Table I. For the low porosity samples, the coefficients are higher using Q_{bv}. This confirms that Q_{bv} contains the correct porosity dependence (i.e., none). The correlation coefficients for the higher porosity data set are not significantly different. This is due to the extremely narrow range in the porosities present in this sample set (7 of the 8 samples are within one porosity unit of 20 percent porosity).

Porosity Dependence of the Geometric Term($\Delta \varepsilon_g$)

Another significant result of the fits is that the intercepts are larger for the higher porosity samples. This intercept which is the response of an "equivalent" clean sandstone is porosity dependent. This implies that it is due to a Maxwell-Wagner type polarization.[10] Maxwell-Wagner effects are due to charges accumulating at regions of conductivity variation in the sample. This magnitude of the effect depends on the details of the interface and the volume ratio of the two materials. But not on the surface area involved. This is consistent with a linear porosity dependence in the equation.

This porosity dependence is easily included in the equation:

$$\Delta \varepsilon = \varepsilon_q Q_{bv} + \varepsilon_\varphi \varphi \qquad (10)$$

The results of fits to equation (10) are also given in Table I. These fitted values are obtained from a fit to the entire sample set (27 samples). The high degree of correlation found shows that both the low and the high porosity data can be explained by Equation (10). A linear fit to the porosity explains the data to within experimental accuracies. This linear dependence is expected from elementary considerations of a Maxwell-Wagner type polarization.[11] This linear porosity dependence has been verified by dielectric measurements performed in carbonates.

The partial regression coefficients $R(\Delta \varepsilon, Q_{bv})$ and $R(\Delta \varepsilon, \varphi)$ included in the table are a measure of the correlation between each independent variable (Q_{bv}, φ) and the dependent variable ($\Delta \varepsilon$). The values of these partial coefficients will necessarily be lower than the value of the total correlation coefficient (R). They are included because they give an indication of the relative importance that Q_{bv} and φ have in determining the value of dielectric constant. At the low salinities these measurements were made the clay term is larger. At higher salinities the geometric term increases relative to the clay term and is relatively more important.

Effects of Salinity and Frequency on the Dielectric Constant

The salinity and frequency dependence of each of the terms in equation (10) are discussed in this section. The sample set used for the salinity dependent measurements consists of total of 49

5

Table I. Results of the fits of dielectric data to Q_{bv} and Q_v.

Q_{bv} Analysis (CEC/Bulk Volume): $\Delta\varepsilon = \varepsilon_q Q_{bv} + \Delta\varepsilon_g$

	Low Porosity			High Porosity		
Frequency	ε_q	$\Delta\varepsilon_g$	R	ε_q	$\Delta\varepsilon_g$	R
200 MHz	59.5±12	.193±.19	.81	52.2±6.3	1.46±.19	.96
47 Mhz	102. ±16	.520±.25	.87	99.7±7.0	2.30±.25	.99
25 Mhz	127. ±19	.944±.30	.88	130. ±8.4	2.94±.25	.99
20 Mhz	138. ±21	1.09 ±.32	.88	143. ±9.0	3.25±.26	.99

Q_v Analysis (CEC/Pore Volume): $\Delta\varepsilon = \varepsilon_q Q_v + \Delta\varepsilon_g$

	Low Porosity			High Porosity		
Frequency	ε_q	$\Delta\varepsilon_g$	R	ε_q	$\Delta\varepsilon_g$	R
200 MHz	4.34±1.2	.397±.20	.71	10.1±1.3	1.47±.19	.96
47 HHz	7.77±1.6	.826±.27	.80	19.2±1.5	2.32±.22	.98
25 MHz	9.81±1.9	1.32 ±.32	.82	25.2±1.8	2.97±.27	.97
20 MHz	10.8 ±2.0	1.48 ±.34	.83	27.6±1.9	3.29±.29	.99

Multilinear Fit (All Samples): $\Delta\varepsilon = \varepsilon_q Q_{bv} + \varepsilon_\phi \phi$

Frequency	ε_q	ε_ϕ	R	$R(\Delta\varepsilon, Q_{bv})$	$R(\Delta\varepsilon, \phi)$
200 MHz	50.4 ± 6.3	6.04 ± .93	.94	.81	.53
47 MHz	96.5 ± 8.2	9.78 ± 1.2	.96	.87	.33
25 MHz	127. ± 9.3	13.0 ± 1.4	.97	.89	.43
20 MHz	140. ± 10.	14.5 ± 1.4	.97	.89	.43

samples from a wide range of lithologies, continuously varying in porosity from 5% to 27% and CEC from 0.0 to 10.0 meq/100 gms. Dielectric measurements were made at .01, .05, .10, .20, .40 and .60 molal in pure NaCl brines. Some of the more shaly samples are were not measured at the lowest salinities because of clay swelling effects. There were also limitations on the maximum conductivity of the sample which the equipment could measure, therefore some of the higher conductivity samples weren't measured at the high salinities.

To analyze the data, the high frequency limit is subtracted to obtain $\Delta\varepsilon$, the dispersion. The dispersion is then fit to equation (10) to obtain ε_q and ε_ϕ. The results of the multilinear fits are summarized in Table II.

The Salinity and Frequency Dependence of the Clay Term(ε_q)

The clay term ε_q, is plotted as a function of frequency and salinity in Figure 5. The decrease in the dielectric dispersion in the plot is explained by the compression of the double layer with increasing salinity. Since the boundary condition appropriate for

Table II. Results of the multilinear fits for ε_q and ε_φ.

Multilinear Fits: $\Delta\varepsilon = \varepsilon_q \cdot Q_{bv} + \varepsilon_\varphi \cdot \varphi$

Frequency	ε_q	ε_φ	R	$R(\Delta\varepsilon, Q_{bv})$	$R(\Delta\varepsilon, \varphi)$
.01 Molal					
200 MHz	54.1+/- 8.9	.79+/- .6	.96	.96	.66
47 MHz	99.7+/- 6.6	4.73+/- .9	.98	.96	.76
25 MHz	129. +/- 8.	8.15+/-1.2	.98	.95	.80
20 MHz	142. +/- 8.	9.68+/-1.3	.98	.95	.80
.05 Molal					
200 MHz	52.2+/- 9.0	2.36+/- .8	.91	.89	.78
47 MHz	89.8+/- 6.6	10.8 +/-1.2	.97	.88	.91
25 MHz	117. +/-17.	17.0 +/-1.7	.98	.87	.93
20 MHz	128. +/-19.	19.3 +/-1.9	.98	.87	.93
.10 Molal					
200 MHz	40.6+/- 4.6	3.55+/-1.3	.92	.90	.67
47 MHz	74.2+/- 5.4	18.2 +/-1.5	.98	.88	.85
25 MHz	96.3+/- 7.1	26.2 +/-2.0	.98	.87	.86
20 MHz	105. +/- 7.0	29.2 +/-2.2	.98	.87	.87
.20 Molal					
200 MHz	29.8+/- 4.8	12.0 +/-1.5	.95	.83	.88
47 MHz	66.3+/- 8.7	26.4 +/-2.6	.97	.85	.90
25 MHz	88.5+/-11.4	35.2 +/-3.4	.97	.85	.90
20 MHz	97.4+/-12.5	38.6 +/-3.8	.97	.85	.90
.40 Molal					
200 MHz	33.4+/- 5.7	17.0 +/-2.1	.95	.82	.88
47 MHz	64.6+/-10.6	37.0 +/-3.9	.96	.81	.90
25 MHz	84.4+/-13.9	48.7 +/-5.2	.96	.81	.90
20 MHz	92.7+/-15.2	53.2 +/-5.7	.96	.81	.90
.60 Molal					
200 MHz	35.3+/-10.1	21.5 +/-4.1	.90	.78	.85
47 MHz	70.2+/-16.3	40.6 +/-6.6	.93	.81	.87
25 MHz	89.8+/-20.2	53.8 +/-8.2	.94	.81	.88
20 MHz	97.7+/-21.8	59.1 +/-8.8	.94	.81	.88

clays is that of constant surface charge density the clay counter-ion mobility should decrease with increasing salinity[12]. Since ε_q is directly related to the clay counter-ion mobility, this decrease in the term with increasing salinity is expected.

At high salinity the clay term is independent of salinity. This is consistent with a Stern layer model for the double layer[13].

7

In a Stern layer model the double layer is limited in its compression. The correspondence of salinity dependence of ε_q with the compression of the double layer indicates that dielectric measurements are directly related to clay-counterion mobility. The polarization of the double layer is proportional to the distance the exchange ions move, which is related to the mobility of the clay counter-ions.

The relation of the low frequency in-phase conductivity to clay counter-ion mobility is different. At low frequencies the "effective mobility" appears to increase with increasing salinity. This is because the conductivity measurements include the coupling effects between the clay counter-ions and the brine.[6] Since clay sites are local and discrete, for the clays to conduct and remain electrically neutral ions in the brine must couple on and off the clays. At low salinities this limits the clay conduction. At high salinities there are enough ions present to fully satisfy this coupling and the clays conduct fully. This mechanism dominates clay conduction effects at low frequency and the effective mobility as measured by the conductivity therefore increases with salinity.

Figure 6 is a log-log plot of the clay term. The slope of data indicates that the frequency dependence of the term is close to $1/\sqrt{\omega}$. This is consistent with a diffusion limited process i.e. a Warburg impedance[14]. If this is the correct interpretation of the data, it indicates the local nature of the polarization. This frequency dependence shifts closer to $1/\omega$ at lower frequencies possibly this is due to moving out of a diffusion limited regime.

The Salinity and Frequency Dependence of the Geometric Term(ε_g)

The results of the fits for ε_g at varying frequency and salinity are found in Figure 8. The fitted proportionality constant ε_g scales with the frequency/brine conductivity as shown in Figure 7. This scaling means that the measurement frequency is divided by the brine conductivity to obtain a "scaled frequency". If the data is plotted versus the scaled frequency the curves measured at different salinities collapse to a single curve. It has been pointed out that the dielectric dispersion in carbonates scales in exactly this way.[15]

A Maxwell-Wagner type polarization is caused by the accumulation of charge at regions of conductivity variation. Charge builds up until an equilibrium charge distribution is established similar to the charging of a capacitor. As the frequency is increased the time available for the polarization to be established decreases and therefore the magnitude of the polarization decrease. The polarization however increases with both the amount of charge available and it's mobility. The brine conductivity is proportional to these. Therefore there is a scaling between frequency and brine conductivity for Maxwell-Wagner polarization. This scaling provides a necessary condition for

identification of this mechanism.

The linear porosity dependence is another clue to the origin of the dispersion. For a Maxwell-Wagner polarization the magnitude of the increase in the dielectric constant is independent of grain size. It does depend linearly on the ratio of the amounts of the rock and brine i.e. the porosity. A linear fit to porosity, fits the data to within experimental accuracies.

A log-log plot of ε_φ against frequency again gives a slope of close to -1/2 for the this term. The frequency dependence will be discussed further in relation to the saturation dependence below.

Summary of brine saturated model

The dielectric constant of clastics is given by:

$$\varepsilon = \varepsilon_q Q_{bv} + \varepsilon_\varphi \, \varphi + \varepsilon_{hfl} \tag{11}$$

Where ε_q and ε_φ are empirically derived parameters from fits to an extensive sample set of clastics. The major contributors to the dielectric constant are the polarization of the double layer and a Maxwell-Wagner type polarization. Although the model describes the sample set extremely well, ε_q and ε_φ are fit to the average behavior of the samples. Refinements can be made by making dielectric measurements on specific cores. This is particularly important in rocks which have complicated pore structures at high salinity.

Saturation Dependence

The porosity and salinity dependence of the dielectric constant imply that the saturation dependence should take a definite form. Saturation dependence is perhaps the most difficult topic in shaly sands. This is true for either the conductivity or for the dielectric response because the distribution of fluids in the sample is important and influenced by many variables. This distribution of fluids is determined by a number of effects including the saturation history and wettability.

A nonuniform distribution will have a large impact. The Maxwell-Wagner effect will dominate if there is a saturation gradient. There is also the impact of wettability on the distribution of fluids. If the brine is disconnected there will be a large component of the dispersion due to the Maxwell-Wagner effect. As a place to start the study of the dielectric constant a water wet system was chosen. The samples were saturated with fluorinert, a non-toxic fully fluorinated hydrocarbon. Use of fluorinert insures a water wet system. The high density of fluorinert (1.9 gms/cc) allows accurate saturation measurements to be made hydrostatically, a distinct advantage in the small samples necessary for dielectric measurements.

9

In Figure 9 sample data for a low porosity shaly sample is shown(ϕ=.07, Q_{bv}=.028). There is very little saturation dependence in this sample. This is consistent with shaliness dominating the dielectric dispersion. Since polarization of the double layer is an extremely local effect, replacing brine with oil should have little effect on the dispersion in this case.

In contrast the dielectric data for a clean sample (ϕ=.215 Q_{bv}=.0056) displayed in Figure 10 shows a significant saturation dependence. The dispersion is due to the Maxwell-Wagner effect which has a porosity dependence. The porosity dependence implies there should be a saturation dependence as well.

The Saturation Model: Analogous to a Porosity or a Salinity Change?

The effect of decreasing the water saturation is to decrease the dispersion. An analogy can be made with either decreasing the porosity or the conductivity of the pore fluid. Both will decrease the dielectric dispersion. The dispersion due to pore geometry including the frequency/brine scaling is:

$$\Delta \varepsilon_g = \varepsilon_\varphi \varphi = \gamma / (\omega / \sigma_w)^{1/2} \varphi \qquad (12)$$

Where γ in this approximation is a frequency independent proportionality constant. Substituting φS_w for φ gives:

$$\Delta \varepsilon = \varepsilon_\varphi \varphi S_w \qquad (13)$$

substituting for $\sigma_w S_w^n$ for σ_w gives:

$$\Delta \varepsilon_g = \gamma / (\omega / \sigma_w S_w^n)^{1/2} \varphi = \gamma / (\omega / \sigma_w)^{1/2} \varphi S_w \qquad (14)$$

comparing (12),(13),(14) for n=2 both substitutions decrease the geometric dispersion linearly with saturation. This symmetry between the frequency scaling and the porosity dependence are important tools in understanding the saturation dependence of the dielectric constant. The implication is that the saturation dependence is a probe of the pore geometry in the sample contributing to the dielectric constant. In general the saturation exponent will be reflected in the frequency dependence through equations (12) through (14). The relation between saturation exponents and frequency dependence is under investigation.

Figure 11 and Figure 12 demonstrate the tradeoff between saturation and the effective conductivity of the pore fluids. The dielectric dispersion as a function of saturation is shown for the sample in Figure 10. The dispersion in this sample is due entirely to the Maxwell-Wagner effect and therefore scales with the effective conductivity of the pore fluid ($\sigma_w S_w^n$) as shown.

In general the saturation dependence of a sample will lie somewhere between that expected for the clay and geometric terms.

The larger the geometric term the larger the saturation dependence. For fresh water shaly sands however the clay term dominates, which implies that the saturation dependence of the dispersion is small. In fresh water shaly sands the dispersion is a direct indicator of shaliness.

CONCLUSIONS

A simple model has been developed to explain the effects of shaliness, porosity, frequency, salinity, and saturation on the dielectric constant of shaly sands. Empirical parameters were obtained that give the response due to clays and pore geometry. These parameters are believed to be quite general since they were obtained from fits to a wide range of sample properties.

The experimental saturation data fits conceptually with the porosity and salinity dependent models. A changing saturation was found to be equivalent to either a porosity change or a change in salinity for the geometric dispersion. The clay term was found to be saturation independent.

In clastics the major application for the dielectric model is thought to be in fresh water shaly sands to simultaneously determine shaliness and saturation. With a two frequency measurement of the dielectric constant to directly measure dispersion, saturation and shaliness may be determined with very little influence of salinity. Because of the insensitivity of the dielectric constant to salinity and the difficulties in interpreting conductivity equations the brine conductivity cannot be solved for in this case.

Interpretations at higher salinity are more difficult. Because of the difficulties of gathering data in the borehole a successful application is more difficult. These interpretations will be complicated by the different depth of investigation and resolution of the different frequency tools. This implies that they are measuring the properties of different rock which may have differing saturations and conductivities due to the effects of invasion. A tool which measures the same formation properties at two frequencies is thought to be necessary for application at higher salinities.

Acknowledgments

1.Jahasz,I. 1979, Normalized Q_v-The Key to Shaly Sand Evaluation Using the Waxman-Smits equation in the Absence of Core Data.,22nd Annual Soc. Prof. Well Log Analysts Logging Symp.,June 23-26,Mexico City,Trans.,I,paper z.

2.Sen, P.N.,Relation of Certain Geometrical Features to the Dielectric Anomaly of Rocks.,Geophysics 46, 1714-1720,1981

3.Sherman, M.M., The Determination of Cementation Exponents Using High Frequency Dielectric Measurements., Paper D,SPWLA 24th Logging Symposium, June 27-30, 1983.

4.Hanai, T. (1968), Electrical Properties of Emulsions, Chapter 5 in Emulsion Science, Academic Press.

5.Stryogyn, A. (1972), Equations for Calculating the Dielectric Constant of Saline Water, IEEE Transactions of Microwave Theory and Techniques, August.

6.Waxman, M.H. and Smits, L.J.M. (1968) Electrical Conductivities in Oil-Bearing Shaly Sands. Trans. AIME, v. 243, Part II, 107-122.

7.Myers, M.T., 1989, Pore Combination Modeling: Extending the Hanai-Bruggeman Equation, Soc. Prof. Well Log Analysts, June 11-14. Trans. paper D.

8.Knight, R.J. and A. Nur, The effect of level of water saturation of the dielectric constant of sandstones, Physics and Chemistry of Porous Media, A.I.P. Conf. Proc. no. 107, 336-345, 1985.

9.Patchett, J.G., An Investigation of Shale Conductivity, SPWLA Sixteenth Ann. Logging Symp, June 4-7, 1975, Paper U.

10.Wagners, K.W.,Eklarung der Dielektrischen Nachwirkungen auf Grun Maxwellscher Vorstellungen: Arch. Electr. v. 2, p.371-387

11.Von Hipple, Dielectrics and Waves, John Wiley and Sons, pps 238-234.

12.van Olpen H., An Introduction to Clay Colloid Chemistry John Wiley & Sons, 1977, pps 202-206.

13.Stern, O. (1924),Zur Theorie der Elektrolytischen Doppelschicht, Z. Elektrochem.,30,508-516.

14.Warburg, E.,1901, Uber die Polarisationscapacitat des Platins:Ann. Phys., v.6, pp.125-135.

15.Kenyon, W.E.(1984), Texture Effects of Megahertz Dielectric Properties of Calcite Rock Samples, J.Appl.Phys., v.55, no. 8,pp.3153-3159.
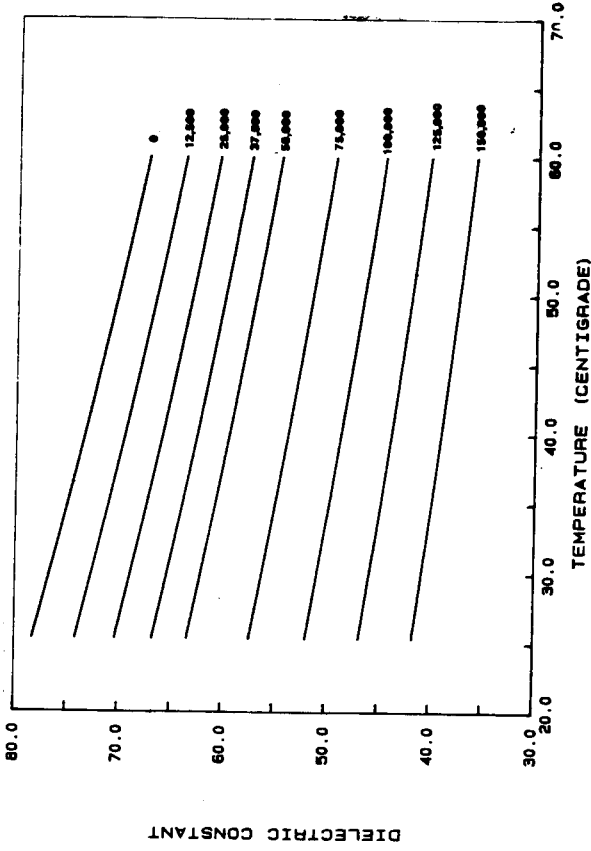
Fig.2 Salinity and temperature dependence
of the dielectric constant of NaCl brine.

Fig.4 Regression of the dielectric
constant on Qbv

Fig.1 Fits of the Hanai-Bruggeman equation
to the high frequency limit data.
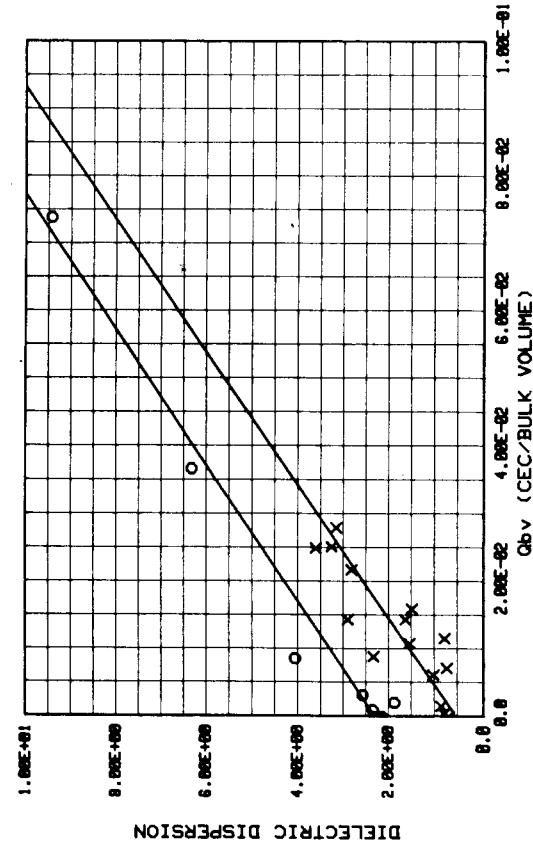
Fig.3 Regression of the dielectric
constant on Qv

13
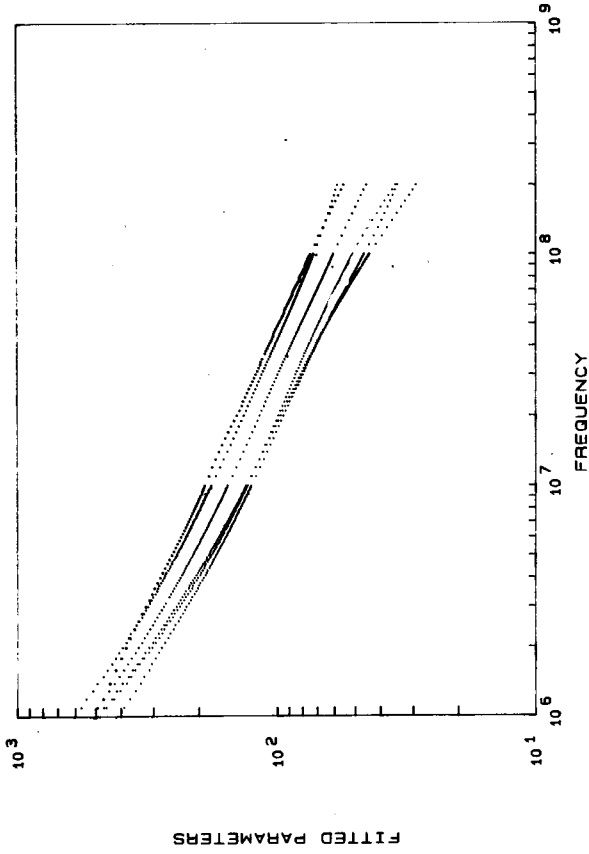
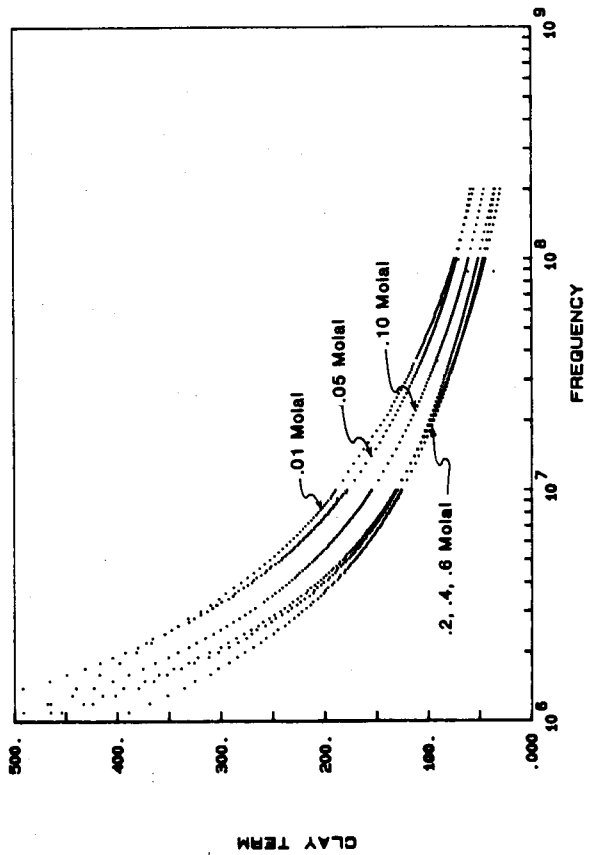Fig.6 Log-Log plot of the clay term. The

slope is -1/2

Fig.8 Scaled geometric term

Fig.5 Clay term as a function of frequency
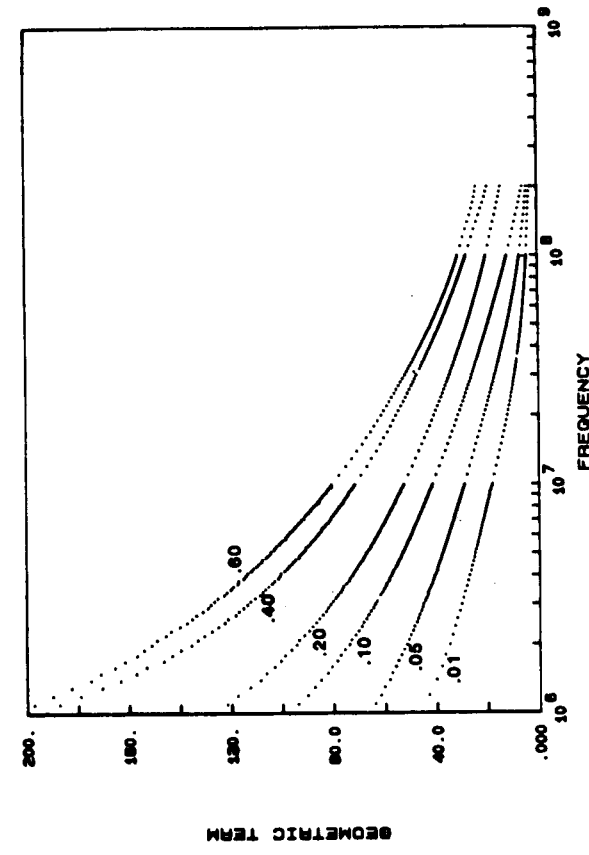
and salinity.

Fig.7 Geometric term as a function of

frequency and salinity

14

Fig.10 Saturation dependence of the dielectric constant for a clean sample.

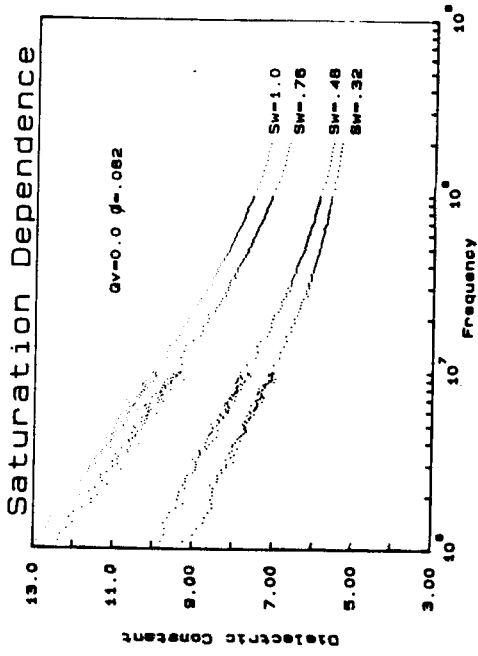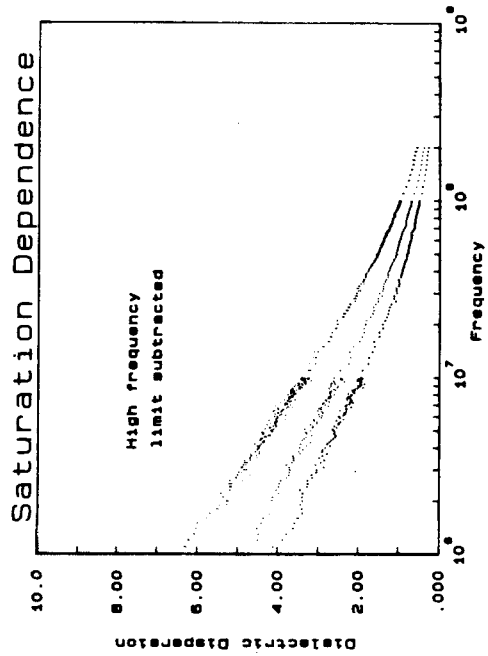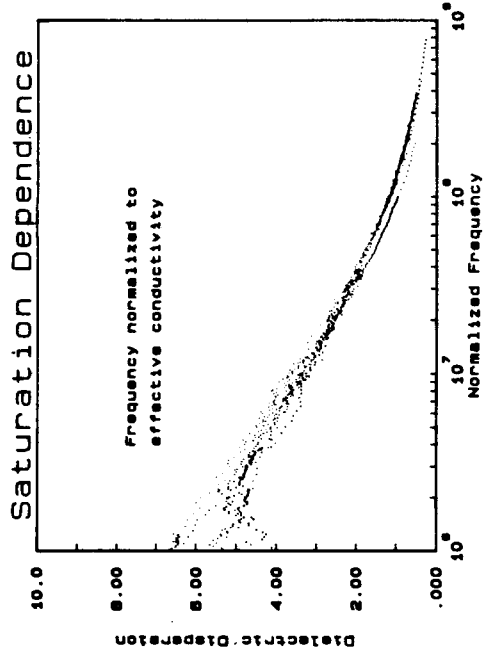Fig.12 Dispersion of a clean sample versus normalized frequency

Fig.9 Saturation dependence of the dielectric constant for a shaly sample.

Fig.11 The dielectric dispersion for a clean sample.

15